Soft Matter

Role of Stefan-Maxwell fluxes in the dynamics of concentrated electrolytes

Journal:	*Soft Matter*
Manuscript ID	SM-ART-06-2018-001222.R1
Article Type:	Paper
Date Submitted by the Author:	19-Jul-2018
Complete List of Authors:	Balu, Bhavya; Carnegie Mellon, Chemical Engineering Khair, Aditya; Carnegie Mellon, Chemical Engineering

Soft Matter

ARTICLE TYPE

Cite this: DOI: 10.1039/xxxxxxxxxx

Role of Stefan-Maxwell fluxes in the dynamics of concentrated electrolytes

Bhavya Balu and Aditya Khair

Received Date
Accepted Date

DOI: 10.1039/xxxxxxxxxx

www.rsc.org/journalname

This theoretical analysis quantifies the effect of coupled ionic fluxes on the charging dynamics of an electrochemical cell. We consider a model cell consisting of a concentrated, binary electrolyte between parallel, blocking electrodes, under a suddenly applied DC voltage. It is assumed that the magnitude of the applied voltage is small compared to the thermal voltage scale, RT/F, where R is the universal gas constant, T is the temperature and F is the Faraday's constant. We employ the Stefan-Maxwell equations to describe the hydrodynamic coupling of ionic fluxes that arise in concentrated electrolytes. These equations inherently account for asymmetry in the mobilities of the ions in the electrolyte. A modified set of Poisson-Nernst-Planck equations, obtained by incorporating Stefan-Maxwell fluxes into the species balances, are formulated and solved in the limit of weak applied voltages. A long-time asymptotic analysis reveals that the electrolyte dynamics occur on two distinct time scales. The first is a faster "RC" time, $\tau_{RC} = \kappa^{-1}L/\mathscr{D}_E$, where κ^{-1} is the Debye length, L is the length of the half-cell, and $\mathscr{D}_E$ is an effective diffusivity, which characterizes the evolution of charge density at the electrode. The effective diffusivity, $\mathscr{D}_E$, is a function of the ambi-polar diffusivity of the salt, $\mathscr{D}_a$, as well as a cross-diffusivity, $\mathscr{D}_{+-}$, of the ions. This time scale also dictates the initial exponential decay of current in the external circuit. At times longer than τ_{RC}, the external current again decays exponentially on a slower, diffusive time scale, $\tau_D \sim L^2/\mathscr{D}_a$, where $\mathscr{D}_a$ is the ambi-polar diffusivity of the salt. This diffusive time scale is due to the unequal ion mobilities that result in a non-uniform bulk concentration of the salt during the charging process. Finally, we propose an approach by which our theory may be used to measure the cross-diffusivity in concentrated electrolytes.

1 Introduction

Electrolytes are prototypical soft matter; thermal fluctuations of ions generate potential differences on the scale of the "thermal voltage," RT/F, where R is the universal gas constant, T is the temperature and F is Faraday's constant. For instance, $RT/F \approx 25mV$ at $T = 298K$. Consequently, the linear response of ion transport in electrolytes can be probed by exposing these materials to applied voltages on the order of RT/F. Indeed, ion transport in electrolytes has been a subject of interest for many decades.[1–7] Practically, the capacitive nature of the electric double layer[1], formed when a charged surface is placed in contact with an electrolyte, is critical in energy storage technologies such as supercapacitors and rechargable batteries.[8–13] Therefore, it is important to quantify the dynamics of double layer charging in electrochemical systems. Characterizing the dynamics of concentrated electrolytes is important in the light of recent studies that have found that concentrated solutions in lithium ion batteries can increase the overall life of the cell.[14,15] There is also interest in using solvent-free electrolytes (e.g., ionic liquids), which are naturally maximally concentrated, in energy storage applications.[16–18] Theoretical predictions that exist for dilute electrolytes need to be modified to predict the behavior of concentrated systems.[19]

A simple, yet instructive, system to study the diffuse charge dynamics that underlie double layer formation is an electrochemical cell containing a binary, initially electro-neutral electrolyte between parallel, blocking, initially uncharged electrodes. The dynamic response of such a model cell to suddenly applied static and alternating voltages has been studied in detail for dilute electrolytes.[2–4,6] When a voltage is suddenly applied across the cell, there is an initial current in the circuit that instantaneously charges the electrodes, thus creating an electric field between them. Microscopically, the ions in the electrolyte, on account of being charged species, gradually migrate in this electric field to oppositely charged electrodes. They form a diffuse layer of charge near the electrodes, which effectively screens the applied potential and causes the initial current to decay. The system reaches a

Department of Chemical Engineering, Carnegie Mellon University, Pittsburgh, Pennsylvania 15213, USA

steady state when the entire applied potential is screened by the ions, and the cell is then said to be charged. Macroscopically, this corresponds to the current in the circuit decaying to zero.

Perhaps the simplest case to consider would be that of a dilute, symmetric electrolyte, where the ions have equal diffusivities, suddenly subject to a DC voltage, V, which is small compared to the thermal voltage, RT/F. Further, it is assumed that the Debye length, κ^{-1}, is much smaller than the length of the half-cell, L, which is typically the experimentally relevant regime. Under these circumstances, the cell can be modeled as an equivalent resistor-capacitor circuit, with the double layers being capacitors and the bulk electrolyte forming a resistor. Calculating the resistance, $R = (\kappa^{-1})^2 L/\varepsilon_r\varepsilon_0\mathscr{D}$, and the capacitance, $C = \varepsilon_r\varepsilon_0/\kappa^{-1}$, one can estimate the time scale for the charging of this cell as the as the time constant for the charging of the R-C circuit, $\tau_{RC} = \kappa^{-1}L/\mathscr{D}$.[3] Here, $\mathscr{D}$ is the common diffusivity of the ions, ε_r is the relative permittivity of the medium, and ε_0 is the permittivity of free space. One could also obtain the charging time scale using microscopic transport models to describe the electrolyte dynamics;[2,4,6] that is, by solving the Poisson-Nernst-Planck (PNP) equations for the spatio-temporal evolution of the concentration of the ions. For dilute electrolytes, it is assumed that the ions are point-sized and do not interact with each other. Therefore, ion transport can be mathematically described by an equation resembling Fick's law, $\mathbf{j}_\pm = m\nabla\mu_\pm$, where $\mathbf{j}_\pm$ is the flux density, m is the mobility, and $\mu_\pm = RT\ln(n_\pm) \pm F\phi$ is the electrochemical potential of the ions,[20] where $n_\pm$ is the number concentration of the ions, and ϕ is the electric potential. Here, '+' represents the cations and '−' represents the anions. Using this equation in a species balance, $\partial n_\pm/\partial t = -\nabla\cdot\mathbf{j}_\pm$, gives the Nernst-Planck equations, which can be solved along with the Poisson equation, $\nabla^2\phi = -\rho/\varepsilon_r\varepsilon_0$, to obtain the concentration profile of the ions, $n_\pm$, and the potential distribution, ϕ. Here, $\rho = e(n_+ - n_-)$ is the total space charge density, and e is the fundamental charge. A detailed historical review and the derivation of the charging time scale for a symmetric, dilute electrolyte is given by Bazant et al.[6] For concentrated systems, where the interactions between ions cannot be neglected, this classic PNP model of dilute electrolytes is of questionable validity. Consequently, there is a need for a more sophisticated description of diffuse charge dynamics in such systems.

There have been two broad contexts in which concentrated solutions have been modeled previously. One approach is to account for the steric interactions between finite sized ions by adding an "excess" term to the electrochemical potential, $\mu_\pm$.[21–24] One could also modify the Poisson equation to account for short-range electrostatic correlations[25,26] In the context of the present problem, there has been interest in studying the dynamics of double layer formation in the presence of ion crowding effects in a cell with a concentrated electrolyte.[21] Similar analysis has also been performed for ionic liquids where there is no solvent.[27] In these analyses, the flux of each species was assumed to depend only on its own electrochemical potential gradient, and the diffusivities of the ions were assumed to be equal, for simplicity.

In the second approach to modelling concentrated electrolytes, the general equations for multi-component diffusion, $\mathbf{j}_i = \sum_j \mathscr{L}_{ij}\nabla\mu_j$, where $\mathscr{L}_{ij}$ are phenomenological coefficients that satisfy Onsager's reciprocal relations[28] and i and j can be '+' (cation) or '−' (anion), have been incorporated into the species balance equations.[20,29] Here, the flux of one species, $\mathbf{j}_\pm$, is dependent on the thermodynamic driving forces, $n_\pm\nabla\mu_\pm$, of all the other species in the system. The general equation for multicomponent diffusion can also be written in the form of Stefan-Maxwell fluxes,[30] which balance the thermodynamic driving force on an ion with the total hydrodynamic drag on it. In this form, as elaborated in section 2, there is an explicit coupling between the ions characterized by a cross diffusivity, $\mathscr{D}_{+-}$. Further, the Stefan-Maxwell fluxes inherently account for the asymmetry in the mobilities of the ions. In the studies that use this approach, there is no external electric field. Thus, every point in the solution is electrically neutral; there is no double layer formation. This theory has largely been used to obtain transport coefficients like the ambi-polar diffusivity and conductivity of the neutral salt in a concentrated solution.[31,32]

There has also been a handful of recent papers on the role of Stefan-Maxwell fluxes in double layer charging. Pstalis and Farrel[33–35] have formulated and numerically solved modified PNP equations similar to those used in the current work that include Stefan-Maxwell fluxes for binary and ternary electrolyte salts (corresponding to three and four component systems), using transport coefficients from an independent molecular dynamics simulation. Gavish et al[36] have developed a framework that includes Stefan-Maxwell coupling as well as short-range steric interactions, which describes different equilibrium structures of the bulk solution and the diffuse layer for a wide range of concentrations and size asymmetries of the ions in the electrolyte. Their framework is able to predict the shift in electric potential from a monotonous decay to decaying oscillations due to over-screening, and, finally, a spatio-temporal instability characterized by non-decaying oscillations of the potential in the cell.

Here, we formulate modified PNP equations that account for coupled ionic fluxes in concentrated electrolytes, through the Stefan-Maxwell equations for multi-component diffusion. These modified PNP equations are subsequently linearized to enable an analytical (as opposed to numerical) solution of the dynamics of double-layer formation and the charging time scale for our model cell. Our analytical approach yields significant physical insight into the impact of Stefan-Maxwell fluxes on double charging. Specifically, two distinct time scales arise from the solution, which characterize the evolution of the external current across the cell. The first is an RC time, $\kappa^{-1}L/\mathscr{D}_E$, where $\mathscr{D}_E$ is an effective diffusivty which accounts for the effect of the cross fluxes between the anion and the cation. Additionally, accounting for the difference in the mobility of ions introduces a slower decay of the current on the diffusive time scale, $L^2/\mathscr{D}_a$, where $\mathscr{D}_a$ is the ambi-polar diffusivity of the salt. This diffusive time scale exists for dilute as well as concentrated electrolytes; it arises as the unequal ion mobilities generate a bulk concentration gradient of neutral salt across the cell, which relaxes via diffusion. The Stefan-Maxwell flux equations, the mathematical description of the problem, and the solution procedure are outlined in section 2. The charging dynamics are discussed in section 3. A conclusion is offered in

section 4.

2 Problem formulation

2.1 Stefan-Maxwell fluxes

The Stefan-Maxwell equations relate the thermodynamic forces driving the transport of a particular species to the hydrodynamic drag caused by its motion relative to all the other species in the solution. This approach allows us to explain the effect of coupled ionic fluxes in concentrated solutions while also accounting for the differences in diffusivities of the ions. Here, we have a ternary system containing a binary, monovalent electrolyte with cations (+) and anions (−), and a neutral solvent (0). The Stefan-Maxwell equations for a ternary system are[30]

$$n_+\nabla\mu_+ = \frac{RT}{n_T}\left[\frac{n_0 n_+}{\mathscr{D}_{0+}}(\mathbf{v_0}-\mathbf{v}_+)+\frac{n_+ n_-}{\mathscr{D}_{+-}}(\mathbf{v}_- -\mathbf{v}_+)\right], \qquad (1)$$

$$n_-\nabla\mu_- = \frac{RT}{n_T}\left[\frac{n_0 n_-}{\mathscr{D}_{0-}}(\mathbf{v_0}-\mathbf{v}_-)+\frac{n_+ n_-}{\mathscr{D}_{+-}}(\mathbf{v}_+ -\mathbf{v}_-)\right]. \qquad (2)$$

As a first step, the ions are treated as point charges, therefore, their electrochemical potential resembles that of an ideal mixture. Hence, $n_\pm\nabla\mu_\pm = RT\nabla n_\pm \pm n_\pm F\nabla\phi$, represents the net thermodynamic driving force as the sum of the driving forces for diffusion and electro-migration; $\mathbf{v}_\pm$ is the average local species velocity of the ions; $n_T = n_+ + n_- + n_0$ is the total concentration of the three species and $\mathscr{D}_{ij}$ is the diffusivity of species i with respect to species j (i and j can be '+', '−' or '0').

Equations (1) and (2) are thus linear in the species velocity and hence its flux, $\mathbf{j}_\pm = n_\pm\mathbf{v}_\pm$, and can be solved to give an explicit expression for the flux in terms of the driving forces. This process of rearranging the Stefan-Maxwell equations into the form of the general equations for multi-component diffusion is largely simplified for a ternary system. Equations (1) and (2) are solved assuming that the solvent velocity $\mathbf{v_0}$ is zero. This is a simplifying assumption that is made to enable an analytic solution. The validity of this assumption is discussed further in section 3. The fluxes thus obtained from the Stefan-Maxwell equations are

$$\begin{aligned}\mathbf{j}_+ =& \frac{-n_T\mathscr{D}_{0+}}{n_0RT\left(n_-\mathscr{D}_{0+}+n_+\mathscr{D}_{0-}+n_0\mathscr{D}_{+-}\right)}\\ &\Big\{n_+\mathscr{D}_{0-}RT\left(\nabla n_+ + \nabla n_-\right)\\ &+n_+F\nabla\phi\mathscr{D}_{0-}\left(n_+ - n_-\right)\\ &+n_0\mathscr{D}_{+-}\left(RT\nabla n_+ + n_+F\nabla\phi\right)\Big\},\end{aligned} \qquad (3)$$

and

$$\begin{aligned}\mathbf{j}_- =& \frac{-n_T\mathscr{D}_{0-}}{n_0RT\left(n_-\mathscr{D}_{0+}+n_+\mathscr{D}_{0-}+n_0\mathscr{D}_{+-}\right)}\\ &\Big\{n_-\mathscr{D}_{0+}RT\left(\nabla n_+ + \nabla n_-\right)\\ &+n_-F\nabla\phi\mathscr{D}_{0+}\left(n_+ - n_-\right)\\ &+n_0\mathscr{D}_{+-}\left(RT\nabla n_- - n_-F\nabla\phi\right)\Big\}.\end{aligned} \qquad (4)$$

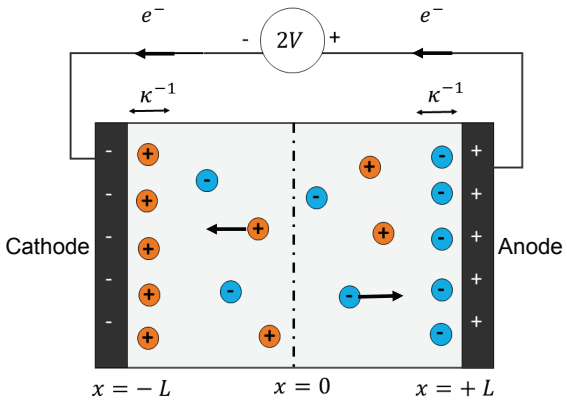

Fig. 1 Schematic of the microscopic response of a model electrochemical cell (of length $2L$) to a suddenly applied voltage of $2V$ at time, $t=0$. Flow of electrons in the external circuit gives rise to an initial current and charges the electrodes. Consequently, ions in the solution form a diffuse layer of charge near the electrodes of width, $\mathscr{O}(\kappa^{-1})$. The bulk solution is electrically neutral.

We now use these fluxes in the species balance equations to solve for the concentration of the ions in the system as a function of space and time. Note that equations (3) and (4) reduce to the fluxes given by Fick's law in the dilute limit, where the ion concentrations n_+ and $n_- \to 0$, and the solvent concentration $n_0 \to n_T$. Further, observe that (3) and (4) introduce an explicit coupling of the flux of one ion to the gradient of the concentration of another. In dilute solutions, this coupling between the concentrations of the anion and cation is implicit through the Poisson equation.

2.2 A model electrochemical cell

We consider a concentrated, binary, monovalent, initially electroneutral electrolyte between parallel, blocking, initially uncharged electrodes, subject to a potential difference of $2V$ imposed at time $t=0$ (figure 1). The species balance equations (5), relate the rate of change of the concentration of an ion, $n_\pm$, to the divergence of its total flux, $\mathbf{j}_\pm$. The Poisson equation for electrostatics (6), which is the differential form of Gauss' Law, relates the space charge density in the solution, $\rho = e(n_+ - n_-)$, to the electric potential, ϕ. Further, the flux of each ion at the (blocking) electrodes is zero and the magnitude of the potential on the electrodes is fixed at V for $t>0$. When the gap between the electrodes, $2L$, is much smaller than the other dimensions of the cell, the ion transport can be assumed to be one-dimensional, in the direction perpendicular to the surface of the electrodes (here, x). Hence, the governing equations are

$$\frac{\partial n_\pm}{\partial t} = -\frac{\partial j_\pm}{\partial x}, \qquad (5)$$

and

$$\frac{\partial^2\phi}{\partial x^2} = -\frac{\rho}{\varepsilon_r\varepsilon_0}; \qquad (6)$$

subject to the boundary conditions (for $t>0$)

$$\phi(x=\pm L,t) = \pm V \quad \text{and} \quad j_\pm(x=\pm L,t) = 0, \qquad (7)$$

and the initial conditions

$$j_{\pm}(x,t=0)=0. \tag{8}$$

Initially, there is no applied potential and the concentrations of the ions are uniform. The fluxes, $j_{\pm}$, are obtained from (3) and (4) by replacing the gradient, ∇f, with a partial derivative, $\partial f/\partial x$, where f represents $\mu_{\pm}$, $n_{\pm}$ or ϕ. Mathematically, this results in a system of partial differential equations for the concentration of the ions and the electric potential within the cell as a function of position and time.

We now non-dimensionalize the governing equations. The scales for concentration, potential, distance, and time are the total concentration, n_T, the thermal voltage, RT/F, length of the half cell, L, and an as yet undefined constant, τ, respectively. The appropriate value of τ will emerge from the subsequent analysis. The dimensionless concentration, potential, distance and time are represented by $\tilde{n}_{\pm}$, $\tilde{\phi}$, $\tilde{x}$ and $\tilde{t}$, respectively. Note that since the concentration of each species is scaled with the total concentration, the dimensionless concentration is the mole fraction of the species. The non-dimensional equations are non-linear and can not be solved analytically; however, in the limit of weak applied voltages, they can be linearized and hence solved. The voltage that is applied is assumed to be small relative to the thermal voltage. Therefore, it is treated as a perturbation from an equilibrium where there is no applied potential. The ratio of this weak applied voltage and the thermal voltage is taken as the perturbation parameter, $\varepsilon = VF/RT$, where $\varepsilon \ll 1$. We pose the following perturbation expansions,

$$\tilde{n}_{\pm} = \tilde{\chi}_{eq} + \varepsilon\tilde{\chi}_{\pm}(\tilde{x},\tilde{t}) + \mathscr{O}(\varepsilon^2), \tag{9}$$

$$\tilde{\phi} = \varepsilon\tilde{\varphi}(\tilde{x},\tilde{t}) + \mathscr{O}(\varepsilon^2). \tag{10}$$

Before the voltage is applied, the mole fractions of the positive and negative ions are equal at all points within the cell to satisfy electro-neutrality; this mole fraction is represented by $\tilde{\chi}_{eq}$. The $\mathscr{O}(\varepsilon)$ change in the mole fraction of the (uncharged) solvent under a weak applied potential is assumed to be negligible and thus the mole fraction of the solvent remains at its equilibrium value, $\tilde{\chi}_0$. The linearized governing equations and corresponding initial and boundary conditions for the $\mathscr{O}(\varepsilon)$ variables, $\tilde{\chi}_{\pm}$ and $\tilde{\varphi}$, obtained using equations (3) to (8) are

$$\frac{L^2}{\tau}\frac{\partial\tilde{\chi}_+}{\partial\tilde{t}} = \frac{\mathscr{D}_{0+}}{\tilde{\chi}_0}\left[\frac{\tilde{\chi}_{eq}\mathscr{D}_{0-}}{\mathscr{D}}\left(\frac{\partial^2\tilde{\chi}_+}{\partial\tilde{x}^2}+\frac{\partial^2\tilde{\chi}_-}{\partial\tilde{x}^2}\right) + \frac{\tilde{\chi}_0\mathscr{D}_{+-}}{\mathscr{D}}\left(\frac{\partial^2\tilde{\chi}_+}{\partial\tilde{x}^2}+\tilde{\chi}_{eq}\frac{\partial^2\tilde{\varphi}}{\partial\tilde{x}^2}\right)\right], \tag{11}$$

$$\frac{L^2}{\tau}\frac{\partial\tilde{\chi}_-}{\partial\tilde{t}} = \frac{\mathscr{D}_{0-}}{\tilde{\chi}_0}\left[\frac{\tilde{\chi}_{eq}\mathscr{D}_{0+}}{\mathscr{D}}\left(\frac{\partial^2\tilde{\chi}_+}{\partial\tilde{x}^2}+\frac{\partial^2\tilde{\chi}_-}{\partial\tilde{x}^2}\right) + \frac{\tilde{\chi}_0\mathscr{D}_{+-}}{\mathscr{D}}\left(\frac{\partial^2\tilde{\chi}_-}{\partial\tilde{x}^2}-\tilde{\chi}_{eq}\frac{\partial^2\tilde{\varphi}}{\partial\tilde{x}^2}\right)\right], \tag{12}$$

and

$$\frac{\partial^2\tilde{\varphi}}{\partial\tilde{x}^2} = -\frac{\kappa^2L^2}{2\tilde{\chi}_{eq}}(\tilde{\chi}_+-\tilde{\chi}_-). \tag{13}$$

At $\tilde{x}=\pm1$ and $\tilde{t}>0$,

$$(\mathscr{D}_{0-}+\mathscr{D}_{+-})\frac{\partial\tilde{\chi}_+}{\partial\tilde{x}}+\mathscr{D}_{0-}\frac{\partial\tilde{\chi}_-}{\partial\tilde{x}}+\tilde{\chi}_{eq}\mathscr{D}_{+-}\frac{\partial\tilde{\varphi}}{\partial\tilde{x}}=0, \tag{14}$$

$$(\mathscr{D}_{0+}+\mathscr{D}_{+-})\frac{\partial\tilde{\chi}_-}{\partial\tilde{x}}+\mathscr{D}_{0+}\frac{\partial\tilde{\chi}_+}{\partial\tilde{x}}-\tilde{\chi}_{eq}\mathscr{D}_{+-}\frac{\partial\tilde{\varphi}}{\partial\tilde{x}}=0, \tag{15}$$

and

$$\tilde{\varphi}=\pm1; \tag{16}$$

and at $\tilde{t}=0$

$$\tilde{\chi}_{\pm}=0. \tag{17}$$

Here, $\mathscr{D}=(\tilde{\chi}_{eq}\mathscr{D}_{0+}+\tilde{\chi}_{eq}\mathscr{D}_{0-}+\tilde{\chi}_0\mathscr{D}_{+-})$ is defined for brevity and can be viewed as a mole-fraction weighted diffusion coefficent. The Debye length is $\kappa^{-1}=\sqrt{\varepsilon_r\varepsilon_0RT/2n_T\tilde{\chi}_{eq}e^2F}$. In the limit of a dilute solution, the mole fraction of the ions $\tilde{\chi}_{eq}\to0$, and that of the solvent $\tilde{\chi}_0\to1$, thereby eliminating the cross fluxes from the species balance equations and recovering the linearized PNP equations for dilute electrolytes.[2,4,6]

The potential, $\tilde{\varphi}$, is eliminated from equations (11) and (12) using (16). The resulting equations are transformed into Laplace space (thus eliminating time) using the definition, $\tilde{G}(\tilde{x},s)=\int_0^{\infty}\tilde{g}(\tilde{x},\tilde{t})e^{-s\tilde{t}}d\tilde{t}$, where s is the Laplace variable and $\tilde{g}(\tilde{x},\tilde{t})$ is a shorthand for $\tilde{\chi}_+$, $\tilde{\chi}_-$, or $\tilde{\varphi}$, whose corresponding representations in the Laplace space are, $\tilde{X}_+$, $\tilde{X}_-$, and $\tilde{\Phi}$. The result is a set of coupled, second order, homogeneous ordinary differential equations (ODEs) for the mole fractions, $\tilde{X}_+$ and $\tilde{X}_-$. These equations are linear, and therefore, can be expressed as a matrix equation, $\tilde{\mathbf{w}}''=\mathbf{A}\tilde{\mathbf{w}}$, where, $\tilde{\mathbf{w}}$ is a column vector containing the (Laplace transformed) mole fractions of the species, $\tilde{\mathbf{w}}''$ represents the second derivative of this vector and $\mathbf{A}$ is a symmetric coefficient matrix for the system. That is,

$$\tilde{\mathbf{w}}=\begin{pmatrix}\tilde{X}_+\\ \tilde{X}_-\end{pmatrix} \quad\text{and}\quad \tilde{\mathbf{w}}''=\begin{pmatrix}\dfrac{d^2\tilde{X}_+}{d\tilde{x}^2}\\ \dfrac{d^2\tilde{X}_-}{d\tilde{x}^2}\end{pmatrix}. \tag{18}$$

The elements of $\mathbf{A}$ are,

$$\begin{aligned} A_{11} &= s\frac{L^2\left(\tilde{\chi}_{eq}\mathscr{D}_{0+}+\tilde{\chi}_0\mathscr{D}_{+-}\right)}{\tau\mathscr{D}_{+-}\mathscr{D}_{0+}}+\frac{\kappa^2L^2}{2},\\ A_{12} &= A_{21} = -s\frac{L^2\tilde{\chi}_{eq}}{\tau\mathscr{D}_{+-}}-\frac{\kappa^2L^2}{2},\\ A_{22} &= s\frac{L^2\left(\tilde{\chi}_{eq}\mathscr{D}_{0-}+\tilde{\chi}_0\mathscr{D}_{+-}\right)}{\tau\mathscr{D}_{+-}\mathscr{D}_{0-}}+\frac{\kappa^2L^2}{2}. \end{aligned} \tag{19}$$

To solve this system of ODEs, we first decouple the equations by diagonalizing the matrix $\mathbf{A}$ using an eigenvalue decomposition, $\mathbf{A}=\mathbf{PDP^{-1}}$, where $\mathbf{D}$ is a diagonal matrix whose elements are the eigenvalues of $\mathbf{A}$, and $\mathbf{P}$ is a matrix whose columns are the corresponding eigenvectors. The two eigenvalues, λ_i, are given

by

$$\lambda_i = \frac{Tr(\mathbf{A}) \pm \sqrt{(Tr(\mathbf{A}))^2 - 4\,(Det(\mathbf{A}))}}{2}; \tag{20}$$

and the corresponding eigenvectors, $\mathbf{v}_i$, are

$$\mathbf{v}_i = \begin{pmatrix} \dfrac{A_{11} - A_{22} \pm \sqrt{(Tr(\mathbf{A}))^2 - 4\,(Det(\mathbf{A}))}}{2A_{12}} \\ \\ 1 \end{pmatrix}. \tag{21}$$

Here, $i = 1$ and 2, correspond to taking the positive and the negative signs in (20) and (21), respectively. Here, $Tr(\mathbf{A}) = A_{11} + A_{22}$, is the trace of the matrix, and $Det(\mathbf{A}) = A_{11}A_{22} - A_{12}A_{21}$, is its determinant. Now, we define a transformed vector of mole fractions, $\tilde{\mathbf{u}} = \mathbf{P}^{-1}\tilde{\mathbf{w}}$. Since the matrix $\mathbf{P}^{-1}$ is a constant in space, $\tilde{\mathbf{u}}'' = \mathbf{P}^{-1}\tilde{\mathbf{w}}''$. The system of ODEs in the transformed variable, $\tilde{\mathbf{u}}$, becomes $\tilde{\mathbf{u}}'' = \mathbf{D}\tilde{\mathbf{u}}$. Since $\mathbf{D}$ is a diagonal matrix, the equations for $\tilde{\mathbf{u}}$ are decoupled and are hence straightforward to solve. Once we have a solution for $\tilde{\mathbf{u}}$, the original vector of mole fractions, $\tilde{\mathbf{w}}$ is simply given by $\tilde{\mathbf{w}} = \mathbf{P}\tilde{\mathbf{u}}$. In this manner, the mole fractions in Laplace space can be expressed as

$$\tilde{X}_+ = v_1\alpha_1 \sinh\left(\sqrt{\lambda_1}\tilde{x}\right) + v_2\alpha_2 \sinh\left(\sqrt{\lambda_2}\tilde{x}\right), \tag{22}$$

$$\tilde{X}_- = \alpha_1 \sinh\left(\sqrt{\lambda_1}\tilde{x}\right) + \alpha_2 \sinh\left(\sqrt{\lambda_2}\tilde{x}\right). \tag{23}$$

Here, λ_1 and λ_2 are the eigenvalues and v_1 and v_2 are the first elements of the corresponding eigenvectors of matrix $\mathbf{A}$. Since the cations and anions have an equal magnitude of charge and the cathode and anode have the same magnitude of applied potential, we expect the distribution of charge density in the cell to be anti-symmetric. We have made use of this property to express the solutions as hyperbolic sines in (22) and (23). The coefficients, α_1 and α_2, can be found from the two boundary conditions that the flux of each species is zero at the electrode. To evaluate the flux, we also require that the $\mathscr{O}(\varepsilon)$ value of the potential at the anode is held constant and equal to unity. Hence, the coefficients are

$$\alpha_1 = \frac{s^{-1}\,\mathrm{sech}\,\sqrt{\lambda_1}}{Q}, \tag{24}$$

and

$$\alpha_2 = -\frac{\sqrt{\lambda_1}\cosh\sqrt{\lambda_1}}{\sqrt{\lambda_2}\cosh\sqrt{\lambda_2}}\left(\frac{v_1+1}{v_2+1}\right)\alpha_1, \tag{25}$$

where

$$Q = \frac{\kappa^2 L^2}{2\tilde{\chi}_{eq}}\left[\frac{(v_1-1)}{\sqrt{\lambda_1}}\left(1 - \frac{\tanh\sqrt{\lambda_1}}{\sqrt{\lambda_1}}\right)\right.$$

$$\left. - \frac{(v_1+1)(v_2-1)\sqrt{\lambda_1}}{(v_2+1)\lambda_2}\left(1 - \frac{\tanh\sqrt{\lambda_2}}{\sqrt{\lambda_2}}\right)\right]$$

$$- \frac{1}{\tilde{\chi}_{eq}}\left[\sqrt{\lambda_1}\left(v_1 - v_2\frac{v_1+1}{v_2+1}\right)\right].$$

Note that the eigenvalues and eigenvectors, and hence the coefficients, α_i, are functions of the Laplace variable, s. Transformation of this solution back into the time domain can be performed numerically. However, an asymptotic analysis is carried out to extract the time scale for the long-time behaviour of the solution. This time scale is representative of how long the cell takes to charge, that is, for the ions to screen the applied potential completely. We study the evolution of three quantities in particular: the charge density at the anode; the salt concentration at the anode; and the total current in the external circuit. Each of these are expressed as linear combinations of the concentration of the ions. For a binary, monovalent electrolyte the $\mathscr{O}(\varepsilon)$ charge density is defined as $\tilde{\rho} = \tilde{\chi}_+ - \tilde{\chi}_-$; and the salt concentration as $\tilde{c} = \tilde{\chi}_+ + \tilde{\chi}_-$. We define the total external current at any given time as an integral of the net volumetric flux across the cell (see Kornilovitch and Jeon[37]),

$$\tilde{I} = \frac{\partial \tilde{V}}{\partial \tilde{t}} + \int_{-1}^{1}\left(\tilde{j}_+ - \tilde{j}_-\right)d\tilde{x}, \tag{26}$$

where $\tilde{V}$ is the dimensionless external voltage. Since $\tilde{V}$ is suddenly applied, its time derivative contributes to an initial spike in the current. Thus the long time behaviour of the current is the integral of the total volumetric flux over the length of the cell. Using the linearized forms of equations (3) and (4), this integral is

$$\tilde{I} = \beta\left[\mathscr{D}_{0+}\tilde{\chi}_+|_{\tilde{x}=1} - \mathscr{D}_{0-}\tilde{\chi}_-|_{\tilde{x}=1} + (\mathscr{D}_{0+} + \mathscr{D}_{0-})\,\tilde{\chi}_{eq}\right]. \tag{27}$$

Here,

$$\beta = \frac{-2\mathscr{D}_{+-}}{\mathscr{D}_a\mathscr{D}}. \tag{28}$$

We also rewrite the above expression (27) to indicate how the external current relates to the charge density ($\tilde{\rho}$) and the salt concentration ($\tilde{c}$) of the electrolyte.

$$\tilde{I} = \frac{\beta}{2}\left[(\mathscr{D}_{0+} - \mathscr{D}_{0-})\,\tilde{c}|_{\tilde{x}=1} - (\mathscr{D}_{0+} + \mathscr{D}_{0-})\,\tilde{\rho}|_{\tilde{x}=1} + (\mathscr{D}_{0+} + \mathscr{D}_{0-})\,2\tilde{\chi}_{eq}\right]. \tag{29}$$

We examine the behaviour of the $\mathscr{O}(\varepsilon)$ ion concentrations at the anode, $\tilde{X}_+$ and $\tilde{X}_-$, at long times, $t \gg \tau_D$, where τ_D is a diffusive time scale defined as $\tau_D = L^2/\mathscr{D}_a$. In Laplace space, this corresponds to the non-dimensional Laplace variable $s \ll \tau\mathscr{D}_a/L^2$. This analysis yields

$$\lim_{s\to 0}\tilde{X}_+(\tilde{x}=1) \sim \frac{-\tilde{\chi}_{eq}}{s\left(1 + s\dfrac{\kappa^{-1}L\coth\kappa L}{\tau\mathscr{D}_E}\right)} - \frac{\tilde{\chi}_{eq}\tilde{\chi}_0\kappa^{-1}L(\mathscr{D}_{0+} - \mathscr{D}_{0-})\coth\kappa L}{2\tau\mathscr{D}_{0+}\mathscr{D}_{0-}\left(1 + s\dfrac{L^2\tilde{\chi}_0}{3\tau\mathscr{D}_a}\right)}, \tag{30}$$

and

$$\lim_{s\to 0}\tilde{X}_-(\tilde{x}=1) \sim \frac{\tilde{\chi}_{eq}}{s\left(1 + s\dfrac{\kappa^{-1}L\coth\kappa L}{\tau\mathscr{D}_E}\right)} - \frac{\tilde{\chi}_{eq}\tilde{\chi}_0\kappa^{-1}L(\mathscr{D}_{0+} - \mathscr{D}_{0-})\coth\kappa L}{2\tau\mathscr{D}_{0+}\mathscr{D}_{0-}\left(1 + s\dfrac{L^2\tilde{\chi}_0}{3\tau\mathscr{D}_a}\right)}. \tag{31}$$

Here, $\mathscr{D}_E$ is an "effective" diffusivity that arises naturally from the solution, details of which are elaborated in the next section. The expressions (30) and (31) represent the Laplace transform of the sum of two exponential functions and can be expressed as,

$$\tilde{X}_+(\tilde{x}=1) \sim -\frac{\tilde{\chi}_{eq}}{s(1+s\tilde{\tau}_{RC})} - \frac{\gamma}{\kappa L}\frac{\tilde{\chi}_{eq}}{1+s\tilde{\tau}_D} \tag{32}$$

and

$$\tilde{X}_-(\tilde{x}=1) \sim \frac{\tilde{\chi}_{eq}}{s(1+s\tilde{\tau}_{RC})} - \frac{\gamma}{\kappa L}\frac{\tilde{\chi}_{eq}}{1+s\tilde{\tau}_D} \tag{33}$$

Inverting this solution gives the ion concentrations at the anode in terms of the dimensionless time, $\tilde{t}$, as

$$\tilde{\chi}_+(\tilde{x}=1) \sim -\tilde{\chi}_{eq}\left[1-\exp(-\tilde{t}/\tilde{\tau}_{RC}) + \frac{\gamma}{\kappa L}\exp(-\tilde{t}/\tilde{\tau}_D)\right], \tag{34}$$

and

$$\tilde{\chi}_-(\tilde{x}=1) \sim \tilde{\chi}_{eq}\left[1-\exp(-\tilde{t}/\tilde{\tau}_{RC}) - \frac{\gamma}{\kappa L}\exp(-\tilde{t}/\tilde{\tau}_D)\right]. \tag{35}$$

Here,

$$\tilde{\tau}_{RC} = \frac{\kappa^{-1}L\coth\kappa L}{\tau\mathscr{D}_E}, \tag{36}$$

$$\tilde{\tau}_D = \frac{L^2\tilde{\chi}_0}{3\mathscr{D}_a\tau}, \tag{37}$$

$$\gamma = \frac{3\mathscr{D}_a(\mathscr{D}_{0+}-\mathscr{D}_{0-})\coth\kappa L}{2\mathscr{D}_{0+}\mathscr{D}_{0-}}. \tag{38}$$

The long time behaviour of the charge density, the salt concentration and the external current can thus be obtained from equations (34) and (35) as follows. The charge density

$$\tilde{\rho}(\tilde{x}=1) = \tilde{\chi}_+ - \tilde{\chi}_- \sim -2\tilde{\chi}_{eq}(1-\exp(-\tilde{t}/\tilde{\tau}_{RC})); \tag{39}$$

the salt concentration

$$\tilde{c}(\tilde{x}=1) = \tilde{\chi}_+ + \tilde{\chi}_- \sim -2\tilde{\chi}_{eq}\frac{\gamma}{\kappa L}\exp(-\tilde{t}/\tilde{\tau}_D); \tag{40}$$

and the external current

$$\begin{aligned}\tilde{I} &= \beta\left(\mathscr{D}_{0+}\tilde{\chi}_+ - \mathscr{D}_{0-}\tilde{\chi}_- + (\mathscr{D}_{0+}+\mathscr{D}_{0-})\tilde{\chi}_{eq}\right)\\ &\sim \beta\tilde{\chi}_{eq}\Big[(\mathscr{D}_{0+}+\mathscr{D}_{0-})\exp(-\tilde{t}/\tilde{\tau}_{RC})\\ &\quad - \frac{\gamma}{\kappa L}(\mathscr{D}_{0+}-\mathscr{D}_{0-})\exp(-\tilde{t}/\tilde{\tau}_D)\Big].\end{aligned} \tag{41}$$

The minus sign of the charge density in (39) indicates an accumulation of negative charge at the anode. The minus sign of the salt concentration in (40) would indicate a depletion of salt at the anode when $\gamma > 0$ and an accumulation of salt at the anode when $\gamma < 0$. The asymptotic solutions predict that the charge density evolves with an RC time scale, the salt concentration decays with a diffusive time scale; whereas both the RC time and the diffusive time appear in the long time behaviour of the external current.

3 Results and Discussion

From the asymptotic expressions (39), (40) and (41), we see that two different time scales emerge. The first is an RC time, $\tilde{\tau}_{RC}$,

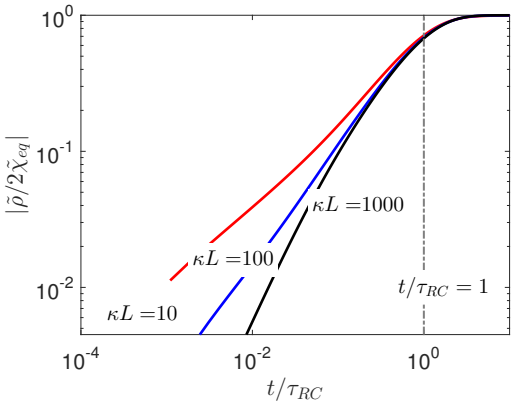

Fig. 2 (a) The evolution of the magnitude of normalized $\mathscr{O}(\varepsilon)$ charge density at the surface of the anode with time for different values of κL. The charge density varies on the RC time, represented by the vertical dashed line. The equilibrium mole fraction of the salt, $2\tilde{\chi}_{eq} = 0.2$, and we take the ratio $\mathscr{D}_{+-}/\mathscr{D}_a = 3.75$.

that characterizes the evolution of the charge density as well as the initial decay of the current. The dimensional RC time τ_{RC} is obtained by factoring out τ from the dimensionless time constant, $\tilde{\tau}_{RC}$. Hence,

$$\tau_{RC} = \tilde{\tau}_{RC}\tau = \frac{\kappa^{-1}L}{\mathscr{D}_E}\coth\kappa L, \tag{42}$$

The RC time scale is similar to that obtained for the charging dynamics for dilute, symmetric solutions.[6] This can be explained by the fact that capacitive double layers are assumed to be formed at equilibrium in both dilute and concentrated systems. The capacitance of the diffuse layer, which depends on its thickness, $\mathscr{O}(\kappa^{-1})$, is an equilibrium property that does not depend on the dynamics of its formation. However, accounting for coupled ionic fluxes in the system through Stefan-Maxwell equations alters the resistance in the bulk solution and hence the value of τ_{RC}. This impact is captured in the effective diffusivity, $\mathscr{D}_E$, defined by

$$\frac{1}{\mathscr{D}_E} = (1-2\tilde{\chi}_{eq})\left(\frac{1}{\mathscr{D}_a} + \frac{1}{\mathscr{D}_{0+}} - \frac{1}{\mathscr{D}_{0-}}\right) + 2\tilde{\chi}_{eq}\frac{1}{\mathscr{D}_{+-}}. \tag{43}$$

Here, $\mathscr{D}_a$ is the ambi-polar diffusivity, defined as $\mathscr{D}_a = 2\mathscr{D}_{0+}\mathscr{D}_{0-}/(\mathscr{D}_{0+}+\mathscr{D}_{0-})$, and $\mathscr{D}_{+-}$ is the cross-diffusivity between the ions. It is also a function of the equilibrium mole fraction of the salt, $2\tilde{\chi}_{eq}$. For a dilute, symmetric electrolyte, where $2\tilde{\chi}_{eq} \to 0$, and $\mathscr{D}_a = \mathscr{D}_{0+} = \mathscr{D}_{0-}$, the effective diffusivity reduces to the common diffusivity of the ions.

The second time scale, $\tilde{\tau}_D$, represents the long time decay of the salt concentration and the external current. The dimensional diffusive time is

$$\tau_D = \tilde{\tau}_D\tau = \frac{L^2\tilde{\chi}_0}{3\mathscr{D}_a}. \tag{44}$$

The ratio of the two time scales, τ_D/τ_{RC}, is proportional to κL. For thin Debye layers, $\kappa L \gg 1$, we have $\tau_D \gg \tau_{RC}$. The longer, diffusive time scale arises due to the difference in diffusivities of the ions and can be viewed as a residual effect of the charging process. The positive and negative ions experience the same electric field and they move towards oppositely charged electrodes. Since they have different mobilities, one type of ions migrates

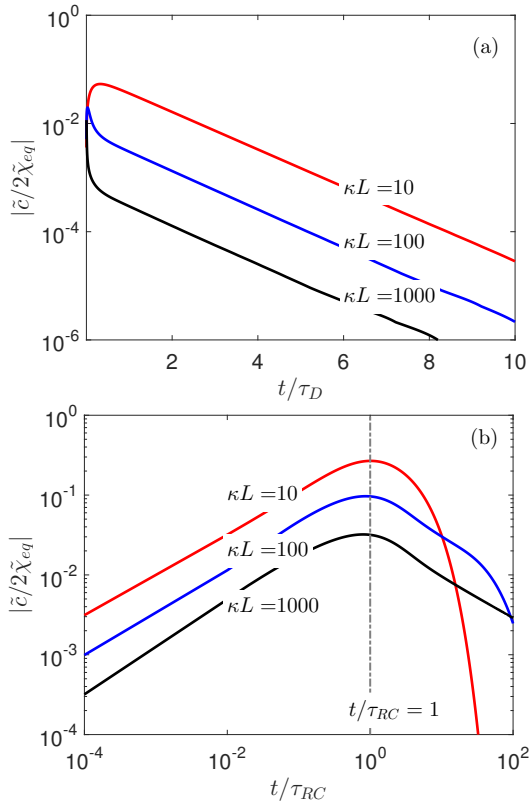

Fig. 3 The evolution of the magnitude of normalized $\mathcal{O}(\varepsilon)$ salt concentration at the anode for different values of κL at (a) times comparable to a diffusive time; and (b) times comparable to RC time . The figures indicate that the initial dynamics of the salt concentration occur on the RC time and the long time decay is on the diffusive time. Here, $2\tilde{\chi}_{eq}=0.2$, $\mathscr{D}_{+-}/\mathscr{D}_a=3.75$, and $\gamma/\coth(\kappa L)=-1$.

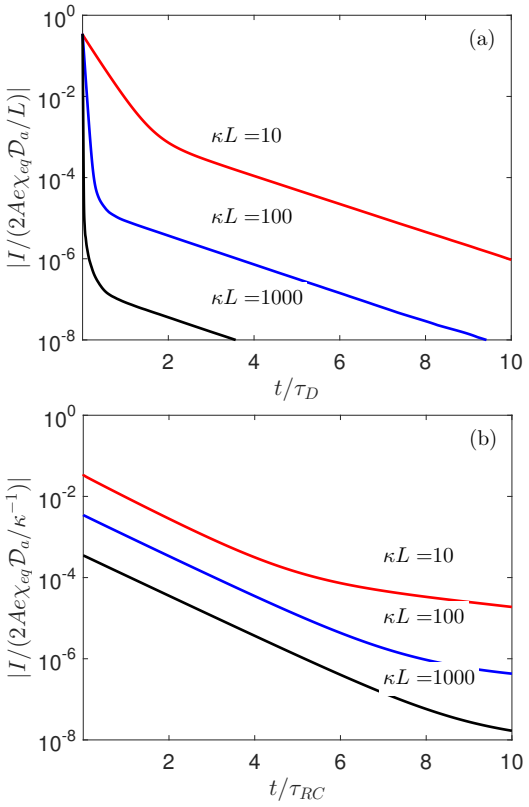

Fig. 4 Evolution of the magnitude of $\mathcal{O}(\varepsilon)$ current in the external circuit for different κL, scaled with (a) the slow diffusive time and (b) the faster RC time. The figure shows the current initially decays on the RC time followed by a decay on the diffusive time. Here, $2\tilde{\chi}_{eq}=0.2$, $\mathscr{D}_{+-}/\mathscr{D}_a=3.75$, and $\gamma/\coth(\kappa L)=-1$.

faster than the other towards their corresponding electrodes. This causes the salt concentration, defined as the sum of the ion concentrations, to vary in the bulk. Once the charging is complete, the ions are in a concentration gradient without an electric field. This concentration gradient driven ion transport is due to diffusion and thus occurs on a diffusive time scale. This residual variation in the bulk concentration is also reflected in the long-time decay of the external current.

Mathematically, this residual effect is captured by the factor $\gamma/\kappa L$. Here, γ (38) is an $\mathcal{O}(1)$ number proportional to the difference in the diffusivities of the ions with respect to the solvent, $\mathscr{D}_{0+}-\mathscr{D}_{0-}$, and thus the diffusive exponential decay is identically zero for symmetric electrolytes and there is no bulk concentration gradient. Further, in the practically prevalent limit of thin Debye layers, $\gamma/\kappa L \ll 1$; therefore, the dynamics are initially dominated by the RC decay. At longer times ($t \gg \tau_{RC}$), the first exponential function in (41) becomes vanishingly small and the current evolution is dominated by the second exponential decay with a diffusive time scale.

To verify that the evolution of the $\mathcal{O}(\varepsilon)$ ion dynamics are on the order of the predicted time scales, the expressions (39), (40) and (41) were compared to a numerical solution. Equations (11), (12) and (16) were solved in MATLAB using an in-built PDE solver, pdepe. The results of the calculation have been plotted for different values of κL, in figures 2, 3 and 4. The magnitude of charge density at the anode increases monotonically and reaches its steady state value on a time scale of order τ_{RC}, as predicted by the asymptotic solution (39); this is demonstrated in figure 2. The steady state value of the charge density depends only on the equilibrium salt mole fraction; it is independent of the ratio κL. Hence, changing the length of the electrolytic cell without changing the concentration of the electrolyte will not affect the equilibrium charge density at the electrodes. The dynamics of the salt concentration are shown in figure 3 (a) and (b). We see a long time exponential decay on the diffusive time scale $\tilde{\tau}_D$ (figure 3(a)); in agreement with the asymptotic prediction (40). Note that the $\mathcal{O}(\varepsilon)$ perturbation of the salt concentration would be identically zero at all times for an electrolyte in which ions have equal diffusivities.[6] Even though the charge density and the salt concentration at the electrode are useful in gaining an understanding of the microscopic charging dynamics, the current in the external circuit is the experimentally measurable quantity. The long time asymptote (41) suggests that the current is a sum of two distinct exponential decays. This can be observed in the numerical solution in figures 4 (a) and (b). In figure 4 (a), the current is plotted against time that has been scaled by the diffusive time, τ_D. The straight lines with slopes independent of the ratio κL indicate the long time exponential decay is on the diffusive time. Similarly, figure 4 (b) is a plot of the current against

time that is scaled with the RC time, τ_{RC}. The initial RC decay is clearly shown by the parallel straight lines at short times.

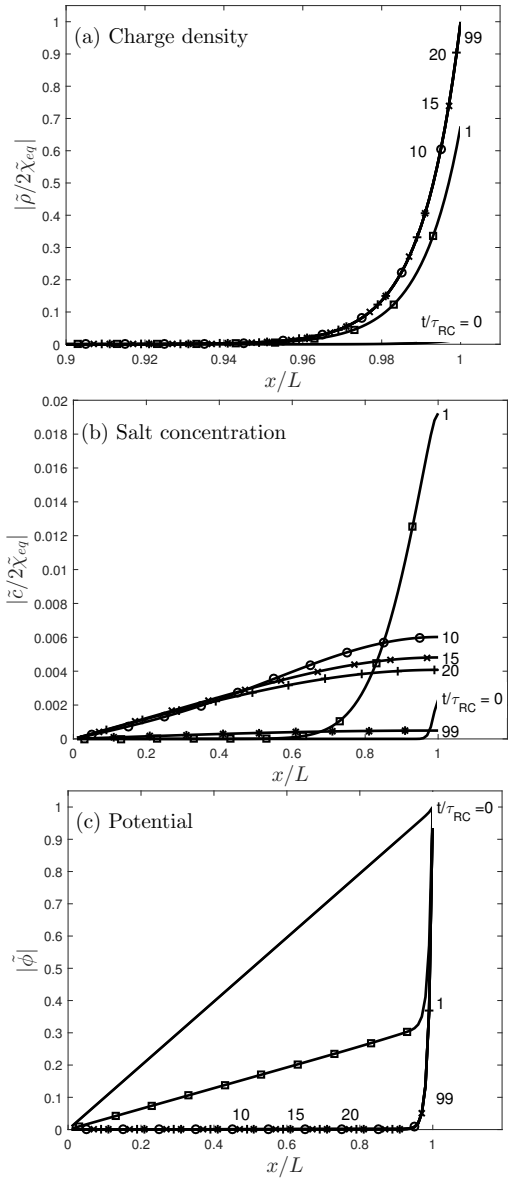

Fig. 5 The evolution of the magnitude of normalized $\mathcal{O}(\varepsilon)$ (a) charge density, (b) salt concentration and (c) potential across the anodic half of the cell at various times t/τ_{RC} (as indicated by the different symbols) for $\kappa L = 100$. This plot demonstrates the charge density and potential have attained equilibrium on the RC time, τ_{RC}, whereas the bulk salt concentration varies on the slower, diffusive time scale, $\tau_D \sim \kappa L \tau_{RC}$.

The variation of the magnitude of the $\mathcal{O}(\varepsilon)$ charge density, salt concentration, and potential across the anodic half of the cell with time are plotted in figures 5 (a), (b) and (c) respectively. For this calculation, we solve equations (11), (12) and (16) in Laplace space and numerically invert the solution into the time domain.[38] Figure 5 (a) shows that after $t > \mathcal{O}(\tau_{RC})$, there is negligible variation in the charge density distribution within the half cell. This reiterates that the charge density indeed reaches its equilibrium value on the RC time. Similarly, figure 5 (c) shows that the potential across the half cell, which is initially linearly varying along the length of the cell, reaches its equilibrium distribution at $t \sim \mathcal{O}(\tau_{RC})$. Conversely, figure 5 (b) suggests that the salt concentration increases initially followed by a slow decay on the diffusive time scale $\tau_D \gg \tau_{RC}$. Thus the salt concentration continues to evolve after the charge density and the potential across the cell have essentially reached equilibrium. Notably, the salt concentration gradient is transient, since the initial and final states of the cell have zero salt concentration gradients in the bulk electrolyte outside the Debye layers.

The predicted time scales should be valid beyond the specific situation of a suddenly applied voltage that is considered here. For instance, the inverse of the time scales would be the characteristic frequencies of double layer charging under an ac voltage, as employed in electrochemical impedance spectroscopy (EIS).[39,40] In particular, the long time diffusive decay of the current would correspond to the low frequency behavior of the impedance. However, this is distinct from the more familiar Warburg impedance due to bulk concentration gradients arising from chemical reactions at the electrodes, since in our system, the electrodes are blocking and there is no salt gradient at steady state.

We now return to the assumption of zero solvent velocity in equations (3) and (4). We do not expect the relaxation of this assumption to essentially alter the charging dynamics we predict, for the following reason. Following the arguments of Psaltis and Farrel[35], a zero solvent velocity would mean that electric body force on a fluid element (equal to product of local electric field and net ionic charge density) is balanced by a pressure gradient to maintain mechanical equilibrium. This pressure gradient could generate additional ionic fluxes for a non-ideal system where volume changes due to mixing are taken into account.[33,35] However, these pressure-driven fluxes would only arise in regions containing a net charge density. In the thin-double-layer limit, such regions are confined to very close to the electrode surface, whereas the bulk of the electrolyte is electro-neutral. Hence, the pressure-driven fluxes do not affect the ion transport across the electroneutral majority of the cell; it is this cell-scale transport that determines the charging time-scales we derive. This assumption of zero solvent velocity would be questionable for systems where the thickness of the Debye layer is comparable to the length of the cell, and also for large applied potentials.

Our analysis suggests a method by which to infer the cross diffusivity $\mathscr{D}_{+-}$ from the current evolution under a suddenly applied voltage. Specifically, the short time and long time exponential decay of the current allow one to infer the RC time scale, τ_{RC}, and the diffusive time scale, τ_D, respectively. From the expression for the diffusive time scale (44), it is then possible to infer the ambipolar diffusivity, $\mathscr{D}_a$ of the salt. Further, given the diffusivity of the ions with respect to the solvent, $\mathscr{D}_{0+}$ and $\mathscr{D}_{0-}$, using the expressions for the RC time scale (42) and the effective diffusivity (43), it would be possible to infer the cross diffusivity of the ions.

4 Conclusion

We developed modified PNP equations that account for coupled ionic fluxes in concentrated electrolytes, using which, we derive the time scales for the charging of a model electrochemical cell. The electrolyte dynamics evolve on two distinct time scales: an

RC time that dictates the evolution of the charge density, and a diffusive time, which arises due to an asymmetry in the mobilities of the ions. The effect of coupled ionic fluxes, characterized by the cross-diffusivity, $\mathscr{D}_{+-}$, is apparent only in the shorter RC time whereas the longer diffusive time solely depends on the ambipolar diffusivity of the salt. A natural extension would be apply the modified PNP equations accounting for Stefan-Maxwell fluxes to electrochemical processes in more than one spatial dimension. However, in these cases, the assumption of stationary solvent becomes questionable and care must be taken when coupling the PNP equations to those governing fluid flow. Finally, our modification of the PNP equations could also be used as a complement to previously developed modifications[19] that account for steric effects and electrostatic correlations in concentrated systems.

5 Acknowledgements

The authors acknowledge NSF CAREER support under CBET-1350647.

References

1 D. L. Chapman, *The London, Edinburgh, and Dublin philosophical magazine and journal of science*, 1913, **25**, 475–481.
2 H.-C. Chang and G. Jaffé, *The Journal of Chemical Physics*, 1952, **20**, 1071–1077.
3 J. R. MacDonald, *Transactions of the Faraday Society*, 1970, **66**, 943–958.
4 J. R. Macdonald, *Physical Review*, 1953, **92**, 4.
5 A. Kornyshev and M. Vorotyntsev, *Electrochimica Acta*, 1981, **26**, 303–323.
6 M. Z. Bazant, K. Thornton and A. Ajdari, *Physical review E*, 2004, **70**, 021506.
7 R. F. Stout and A. S. Khair, *Physical Review E*, 2015, **92**, 032305.
8 F. Béguin, V. Presser, A. Balducci and E. Frackowiak, *Advanced materials*, 2014, **26**, 2219–2251.
9 N.-S. Choi, Z. Chen, S. A. Freunberger, X. Ji, Y.-K. Sun, K. Amine, G. Yushin, L. F. Nazar, J. Cho and P. G. Bruce, *Angewandte Chemie International Edition*, 2012, **51**, 9994–10024.
10 R. Kötz and M. Carlen, *Electrochimica acta*, 2000, **45**, 2483–2498.
11 V. Etacheri, R. Marom, R. Elazari, G. Salitra and D. Aurbach, *Energy & Environmental Science*, 2011, **4**, 3243–3262.
12 B. Dunn, H. Kamath and J.-M. Tarascon, *Science*, 2011, **334**, 928–935.
13 M. Armand, F. Endres, D. R. MacFarlane, H. Ohno and B. Scrosati, *Nature materials*, 2009, **8**, 621–629.
14 Z. Jianming, L. J. A., K. Alexander, D. Z. Daniel and X. Jie, *Advanced Science*, 2017, **4**, 1700032.
15 D. W. McOwen, D. M. Seo, O. Borodin, J. Vatamanu, P. D. Boyle and W. A. Henderson, *Energy & Environmental Science*, 2014, **7**, 416–426.
16 A. Lewandowski and A. Świderska-Mocek, *Journal of Power Sources*, 2009, **194**, 601–609.
17 M. C. Buzzeo, R. G. Evans and R. G. Compton, *ChemPhysChem*, 2004, **5**, 1106–1120.
18 T. Sato, G. Masuda and K. Takagi, *Electrochimica Acta*, 2004, **49**, 3603–3611.
19 M. Z. Bazant, M. S. Kilic, B. D. Storey and A. Ajdari, *Advances in colloid and interface science*, 2009, **152**, 48–88.
20 J. Newman and K. E. Thomas-Alyea, *Electrochemical systems*, John Wiley & Sons, 2012.
21 M. S. Kilic, M. Z. Bazant and A. Ajdari, *Physical review E*, 2007, **75**, 021503.
22 J. Bikerman, *The London, Edinburgh, and Dublin Philosophical Magazine and Journal of Science*, 1942, **33**, 384–397.
23 M. Sparnaay, *Recueil des Travaux Chimiques des Pays-Bas*, 1958, **77**, 872–888.
24 N. F. Carnahan and K. E. Starling, *The Journal of Chemical Physics*, 1969, **51**, 635–636.
25 M. Z. Bazant, B. D. Storey and A. A. Kornyshev, *Physical Review Letters*, 2011, **106**, 046102.
26 F. H. Stillinger Jr and R. Lovett, *The Journal of Chemical Physics*, 1968, **48**, 3858–3868.
27 H. Zhao, *Physical Review E*, 2011, **84**, 051504.
28 L. Onsager, *Physical review*, 1931, **38**, 2265.
29 E. L. Cussler, *Multicomponent diffusion*, Elsevier, 2013.
30 E. Lightfoot, E. Cussler and R. Rettig, *AIChE Journal*, 1962, **8**, 708–710.
31 J. Newman and T. W. Chapman, *AIChE Journal*, 1973, **19**, 343–348.
32 N. G. Pinto and E. Graham, *AIChE journal*, 1987, **33**, 436–443.
33 S. Psaltis and T. W. Farrell, *Journal of The Electrochemical Society*, 2011, **158**, A33–A42.
34 T. W. Farrell and S. Psaltis, *Physics of Nanostructured Solar Cells*, Nova Science Publishers Inc, 2009, pp. 327–353.
35 S. T. P. Psaltis, *PhD thesis*, Queensland University of Technology, 2012.
36 N. Gavish, D. Elad and A. Yochelis, *The journal of physical chemistry letters*, 2017, **9**, 36–42.
37 P. Kornilovitch and Y. Jeon, *Journal of Applied Physics*, 2011, **109**, 064509.
38 F. R. De Hoog, J. Knight and A. Stokes, *SIAM Journal on Scientific and Statistical Computing*, 1982, **3**, 357–366.
39 B. A. Yezer, A. S. Khair, P. J. Sides and D. C. Prieve, *Journal of colloid and interface science*, 2015, **449**, 2–12.
40 G. Barbero and I. Lelidis, *Physical Review E*, 2007, **76**, 051501.

Electrochemical Cell

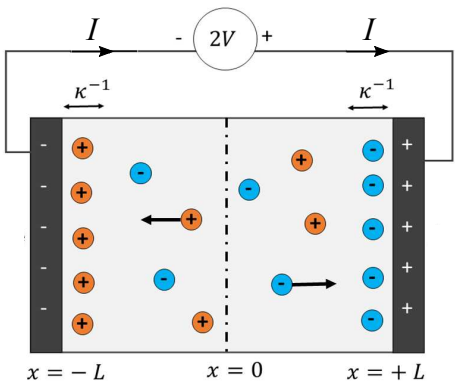

Stefan-Maxwell Ionic Fluxes

External Current